energies

MDPI

Article

Powering the WSN Node for Monitoring Rail Car Parameters, Using a Piezoelectric Energy Harvester

Bogdan Dziadak [1,*], Mariusz Kucharek [1,2] and Jacek Starzyński [1]

[1] Electrical Engineering Department, Warsaw University of Technology, 00-661 Warsaw, Poland; mariusz.kucharek.dokt@pw.edu.pl (M.K.); jacek.starzynski@pw.edu.pl (J.S.)
[2] Łukasiewicz Research Network—Tele and Radio Research Institute, Ratuszowa 11 Street, 03-450 Warsaw, Poland
* Correspondence: bogdan.dziadak@pw.edu.pl; Tel.: +48-222-347-525

Abstract: Monitoring of railroad wagons is important for logistical processes, but above all for safety. One of the key parameters to be monitored is the temperature of the axle box and the bearings in the bogie. The problem with monitoring these parameters is the harsh environment and lack of power supply. In our research, we present a power supply system for a WSN node monitoring the bogie parameters. Knowing the operating conditions, we built a power supply system using a piezoelectric energy harvester. The harvester consists of three piezoelectric elements placed on a double arm pendulum beam. The circuit was modeled in the Comsol Multiphysics environment and then built and tested in laboratory conditions. After confirming energy efficiency, the system was tested on a freight car bogie during an 8 h trip. At typical car vibration frequencies (4–10 Hz), the system is able to generate 73 uW. Combined with an energy buffer of 1000 mAh (3.7 V), it can power a WSN node (based on the nRF5340 chip) for 13 years of operation.

Keywords: energy harvesting; piezoelectric; power unit; freight monitoring

Citation: Dziadak, B.; Kucharek, M.; Starzyński, J. Powering the WSN Node for Monitoring Rail Car Parameters, Using a Piezoelectric Energy Harvester. *Energies* **2022**, *15*, 1641. https://doi.org/10.3390/en15051641

Academic Editor: Abdessattar Abdelkefi

Received: 27 January 2022
Accepted: 21 February 2022
Published: 23 February 2022

1. Introduction

Modern economy, industry and methods of production of goods are highly dependent on a properly functioning supply chain. The transport of goods and people plays a large role in ensuring the proper functioning of logistics processes. Maintenance of the entire transport infrastructure is of significant economic and social importance. One of the elements ensuring its functioning is monitoring and appropriate control. It is particularly visible in railroad transport [1,2], both passenger and freight. One of the key parameters is the safety of rolling stock and passengers. Safety is determined by many factors such as the quality of the railroad infrastructure and the technical condition of locomotives and wagons. One of the problems associated with the operation of railcars is the condition of bearings and axle box of the railcar. Due to high loads, there is a high risk of bearing damage which leads to a rapid temperature rise of the axle box and bogie axle and eventually can lead to wheel breakage and derailment. Therefore, monitoring the axle box temperature gives information about the current state of the bearings and allows to predict the need to replace them. This helps to avoid railroad disasters, as well as costly repairs by mobile services.

Our paper focuses on research on developing a power supply system for a WSN node operating aboard a railcar. The node will measure the temperature of the bearings and axle box in the bogie of a freight car. Electric power supply in freight cars is practically non-existent, so the node will be equipped with a power supply system using energy harvesting methods. Knowing the working environment of the node, we applied a kinetic energy converter using a piezoelectric harvester. This harvester is a two-armed pendulum with a length of 11 cm length and an asymmetric mass installed at the extremities. This approach allows to obtain two resonance frequencies (15 Hz and 22 Hz). By approximating the resonance frequencies of the harvester to the vibration frequency of the railroad car,

the power generated by the system can be significantly increased. Typical car vibration frequencies range from 4 to 10 Hz. Under these conditions, the constructed power supply system had an operational power of 60.5 µW. This efficiency together with the 1000 mAh (3.7 V) energy buffer allows to power the WSN for 13.3 years.

The article is further structured as follows: In Section 2, we gave a brief overview of rail infrastructure monitoring systems. We took a close look at power systems that use EH techniques. Since our main solution is based on a piezoelectric element, in Section 3 we presented basic piezoelectric materials with parameters relevant to energy harvesting. Section 4 is the analysis of the mechanical parameters of the harvester and the modeling and simulation of the target system. Section 5 contains the results of testing the real power unit in laboratory conditions and in the target conditions, i.e., in a freight train car. Discussion of the obtained results, their comparison, energy balance and presentation of potential use, are presented in Section 6. A summary of the research is presented in Section 7.

2. State of the Art

Monitoring and control systems allow maintaining train traffic, give the possibility of detection and prediction of damage, and allow to guarantee the required level of safety. Monitoring systems in this area can be divided into two groups:

- Ground-based systems, characterized by the fact that measuring systems are located on or near the rails. The sections of monitored routes can be different and vary from several tens of meters to several tens of kilometers. The data are usually transmitted using wired/fiber optic interfaces and then via long distance links to the central controller/server of the system. Such systems monitor the condition of tracks and turnouts, but also parameters of passing trains. The monitored train does not have the additional elements of the measurement system. This makes it possible to monitor all trains passing along a given route, and thus to carry out tests on a large number of cases.
- On-board systems are characterized by the fact that the measuring equipment, as well as the first system controller, is installed on board the train. These systems mainly operate as WSNs. They are dominated by short and long range wireless interfaces. In these systems, technical parameters of the train/car or of the freight transported are mainly monitored, less often track parameters. The monitored train is tested over a period of time on different routes. In this way it is possible to collect information about the train parameters under typical operating conditions.

The element that affects the lifetime in both types of systems is the power unit. Therefore, we will analyze the power systems in the above-mentioned systems

In the case of ground-based systems, the energy to power them is drawn from the power grid [3] or battery [4]; in some systems, the energy is transmitted via fiber optic link [5]. However, some ground-based systems use energy harvesting to power the nodes that monitor railroad infrastructure [6]. There are also solutions for universal power systems. One of them is a system that uses the vibrations of a loaded piezoelectric beam mounted on railroad tracks. Vibrations during the passage of a train and especially the moment of passage of a carriage bogie gave the possibility to obtain power equal to 4.9 mW [7]. While in [8], a matrix of 16 piezoelectric PZT harvesters was installed on a railroad sleeper which allowed to achieve power from 81 to 1300 µW. Piezoelectric solution was also used to power a node measuring track vibration in a tunnel in Germany [9]. In this solution, 395 µJ was stored after each train passage. While a system using a piezoelectric beam mounted on the bottom of the rails was presented in [10]. This system generated power of about 1 mW. Similar solutions of piezoelectric harvesters mounted on rails or railroad sleepers are presented in [11–13].

The problem of power supply for measuring nodes in railroad vehicles is important because all devices operating on board a railroad vehicle must meet restrictive safety standards [14]. Any disturbance of the train's power network is registered and may be the reason why the train is not allowed to move. Additionally, in the case of monitoring freight

cars, the power supply is not present in them. Therefore, there is a noticeable trend in the construction of measuring nodes to separate them from the train installation, and to extend the operation of the node on battery power through the use of appropriate hardware and software solutions [14–17], or the use of energy harvesting (EH) methods.

Focusing attention on measurement systems and nodes implemented in rolling stock and using energy harvesting systems, the WSN presented in [18] can be cited. The measurement nodes of the network are installed on the axles of the carriage and measure temperature, vibration, speed and position of the carriage. The power supply node uses a patented ELVIBR circuit that converts the kinetic energy of vibration into electrical energy using an electromagnetic and piezoelectric system. In contrast, He et al. propose to use a matrix of 16 electromagnetic circuits with a geophone structure for power supply [19]. Another application of the electromagnetic system is proposed in [20], where a harvester is suspended from the underside of a freight car platform and used to support the operation of an electronically controlled pneumatic (ECP) brake system. This system generates as much as 4.6 W and the harvesters operate in a three-phase system. A similar design of the harvester is presented in [21], where the efficiency of 1.3 W was obtained. Another onboard power supply system using an electromagnetic system is presented in [22]. The system is able to generate 100 mW of power under the vibration of a train car moving at 80 km/h. Gao et al., on the other hand, present a specialized system using an electromagnetic harvester "with an inertial pendulum" which has an output of 263 mW [23]. Cho et al. presented a piezoelectric circuit for powering black boxes in a train that has a power density of 40 $\mu W/cm^3$ [24]. On the other hand, the SUSTRIAL project studied the spring-mass-oscillator in the piezoelectric generator. It generates 2 μW of power but at a relatively high frequency of 80 Hz [25]. In [26], an Eh circuit using a thin piezoelectric film in a multibeam configuration allowing 13 mW generation at a train vibration frequency of 14 Hz is presented. A structurally similar solution was used in the work [27] and installed on a railcar platform. This made it possible to generate up to 15 mW.

Summarizing the above review, one can say that the systems monitoring the railroad infrastructure are its indispensable element. Depending on the needs, these may be systems with measuring nodes working on the ground or onboard. Regardless of the type of system, an important part of the system or measuring node is a power supply block. The power block is responsible for measuring node working time. This parameter is responsible for the economy of the monitoring system implementation. The short operating time of a system makes its costs high and only important scientific or organizational reasons will allow to implement and run such a system. On the other hand, equipping the system with self-sufficient and self-powering measuring nodes increases the economy and reduces organizational efforts related to the replacement of power units. Additionally, the self-powering node does not interfere with the energy structure of the car or train, which is important from the safety point of view. Because of these benefits, there is a noticeable trend towards the use of power supplies using energy harvesting techniques. In the case of on-board systems, techniques for the conversion of kinetic energy into electrical energy are particularly used, with electromagnetic and piezoelectric harvesters leading the way. The power generated, depending on the size and point of installation of the harvester, ranges from hundreds of μW to tens of mW. This power output allows the construction of a measurement node using low energy controllers and radio links.

3. Piezoelectric Effect and Materials

In our research, we focus on piezoelectric energy converters. Using the piezoelectric phenomenon, the vibration energy of the carriage will be converted into eclectic energy.

The simple piezoelectric effect is based on the induction of electric charges on the surface of the crystal and polarization under the action of external forces. The simple piezoelectric effect is presented in Figure 1, showing particles of lead zirconate titanate PZT ($PbZrO_3$ and $PbTiO_3$) ceramic material. The properties of the piezoelectric effect are described by a system of two linear equations describing relations between electrical and

mechanical quantities. The mechanical description of the piezoelectric effect is defined by Hooke's law, which defines the deformation of a body under the influence of an applied force, where the deformation is proportional to the applied pressure, which is represented by the following Equation (1):

$$S = sT \tag{1}$$

S—dimensionless relative strain.
s—susceptibility coefficient.
T—stress [Pa].

The electrical description uses the property of the law of electric induction, which defines the value of the electric field depending on the pressure exerted on the material, which is represented by Equation (2):

$$D = \varepsilon E \tag{2}$$

D—electric induction [C/m^2].
ε—permeability coefficient.
E—electric field strength [V/m].

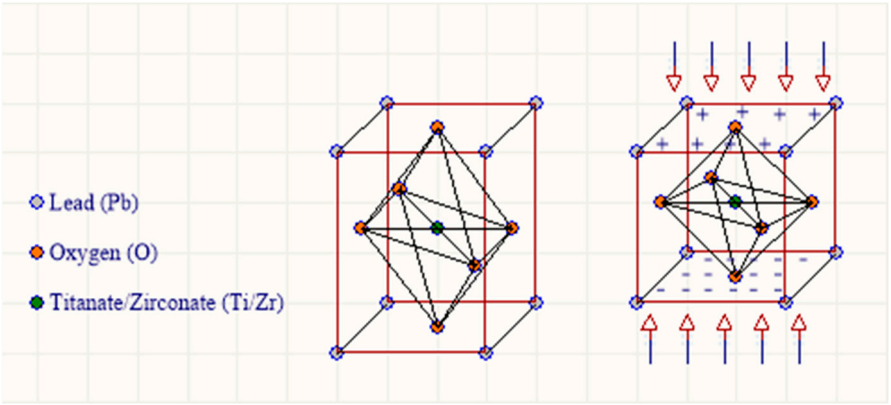

Figure 1. Simple piezoelectric effect on the example of PZT ceramics.

Using the piezoelectric properties of the material, where the deformation and electric induction interact simultaneously, the equations of state are formulated to describe the relationships between the electrical and elastic variables of the medium that occur at certain boundary conditions. The following set of Equation (3) are called the basic equations of electromechanics, where superscript E and T denote the assumed boundary conditions:

$$\begin{cases} S = S^E T + dE \\ D = dT + \varepsilon^T E \end{cases} \tag{3}$$

ε^T—electrical permeability at constant stress T [F/m].
S^E—mechanical susceptibility at constant electric field strength E [Pa^{-1}].
d—piezoelectric effect coefficient.

The amount of energy received can be determined by the efficiency of the designed energy converter. The following equation was used:

$$\eta_{\%} = \frac{P_{OUT}}{P_{IN}} \times 100\% \tag{4}$$

P_{OUT}—electrical output power [W].
P_{IN}—mechanical input power [W].

The inherent phenomenon that characterizes piezoelectric energy converters is the change of electric charge polarization under the influence of mechanical stress direction

change. The rate of polarization change is influenced by three factors: molecular symmetry of the crystal, electrical capacitance of the piezoelectric element, frequency of the stress direction change [28].

There are about 200 piezoelectric materials, but the most popular ones used for energy harvesting can be divided into four main groups presented in Table 1.

Table 1. Classification of piezoelectric materials.

Group	Sample of the Material
Crystals	Seignette's salt, quartz crystals, zinc oxide (ZnO)
Ceramics	Barium titanate ($BaTiO_3$), lead titanate zirconate PZT ($PbZrO_3$ and $PbTiO_3$), potassium niobate ($KNbO_3$)
Polymers	Biopolymers polylactic acid (PLA), polyvinylidene fluoride (biopolymers PVDF)
Polymer composites and nanocomposites	Polyvinylidene fluoride-zinc oxide (PVDF-ZnO), PZT polyimides

The selection of a suitable piezoelectric material for an energy converter depends not only on its piezoelectric properties and application possibilities but also on parameters such as environmental impact, availability and price. Quartz crystals characterized by high efficiency of converting kinetic energy into electrical energy are characterized by high unit price, which often makes it impossible to use them. Quartz and its piezoelectric capabilities are used in the construction of shape change sensors and transducers.

The more often used ceramic materials with high efficiencies, such as PZT [29], are characterized by the presence of lead particles in their structure, which does not have a neutral effect on the environment and is gradually withdrawn from the electronics market. Elements containing a concentration of this element in their structure exceeding 0.1% cannot fulfill the RoHS directive [30]. Barium titanate $BaTiO_3$ is a representative of ceramic materials that do not contain toxic elements, but it is characterized by lower generation efficiency and has all disadvantages characteristic for ceramic elements such as brittleness, high stiffness, lack of flexibility of structure, physical limitations in microcircuits manufacturing.

Piezoelectric polymers are better candidates for piezoelectric energy harvesting applications because they are mechanically flexible, so they can withstand high loads. They also generate sufficient voltage from which sufficient output power can be obtained, they can withstand high electric field strength because they have higher dielectric strength, they have low production cost, and the processing of polymer family materials is easier compared to ceramic materials [31–35].

Polymer composites are formed by combining polymeric and ceramic materials. The main advantage of piezocomposites is the improved electro-mechanical coupling as a result of optimal geometry and elongation of piezoelectric elements in the composites. The high coupling ratio contributes to a broader bandwidth and increased energy transfer. The low acoustic impedance of piezo-composites allows for low-loss energy transfer between the transducers and a propagation medium such as water or tissue. In addition, piezocomposite materials such as MFC (Macro Fiber Composite) can be shaped mechanically, allowing transducers to be made with concave or convex surfaces due to their flexibility [36–38]. PMN-PT material is a solid solution of lead, magnesium and niobium doped with lead titanate oxide $Pb(Mg_{1/3}Nb_{2/3})O_3$-$PbTiO_3$. PMN-PT-based materials are characterized by high dielectric permeability, high piezoelectric properties, and are suitable for applications in multilayer capacitors, actuators, sensors, and electro-optical devices such as piezoelectric motors made with MEMS technology [39].

PZT ceramic materials show the most promising properties for ambient energy harvesting, mainly due to their low resonant frequency. Low operating frequency is desirable because of the brittle structure of ceramic materials [40–42]. Moreover, the PZT material is widely used in industry, for these reasons we used the PZT-5A piezoelectric material.

4. Methodology and Modeling

4.1. Testing Methodology

We begin our research by presenting the operating environment and performance requirements of the target measurement node. Familiarity with the environment and a review of solutions led us to select a harvester geometry. Next, we will present the model and the results of simulation experiments that will initially confirm the feasibility of obtaining a satisfactory power output. After the simulations, we will present the piezoelectric energy harvester realized and tested in laboratory conditions. Then, we will present real-life tests on the target object of the research, i.e., freight wagon bogie. We will discuss the obtained results and present the possibility of using the resulting power source to supply the WSN node monitoring the temperature of the bearings in the axle box.

The adopted methodology has allowed to verify the developed construction of the harvester and the power system already at the stage of simulation and laboratory experiments. Thanks to this, the real tests were carried out as expected.

4.2. Target Working Conditions

The harvester system is designed to operate in the environment of a freight wagon. Regular vibration will come from the rotation of the wheels, and irregular vibration will come from the deformation of the track. Knowing the diameter of the wheel included in the wheelset of the 25TN bogie, which is 920 mm [43], it is possible to calculate the frequency of the train wheel rotation at a speed of 50 km/h and 100 km/h.

$$f = \frac{1}{T} = \frac{V}{\pi d} = \frac{13.88}{(3.14 \times 0.92)} = \sim 4.8 \text{ Hz} \quad (5)$$

$$f = \frac{1}{T} = \frac{V}{\pi d} = \frac{27.77}{(3.14 \times 0.92)} = \sim 9.6 \text{ Hz} \quad (6)$$

f —frequency [Hz].
T—period [s].
V —velocity [m/s].
d—wheel diameter [m].

The harvester should work as close as possible to its resonant frequency to generate the right amount of energy. Operation in resonance is not recommended due to large deflections and possible damage to the device.

Figure 2 shows the assembly diagram of the placement of the system collecting energy from the environment (1) and the communication and measurement sensors (2). A measurement node based on a low-energy controller will collect data from the sensors and, using a wireless interface, will transmit the data with a multi-jump to a controller which will be onboard the locomotive.

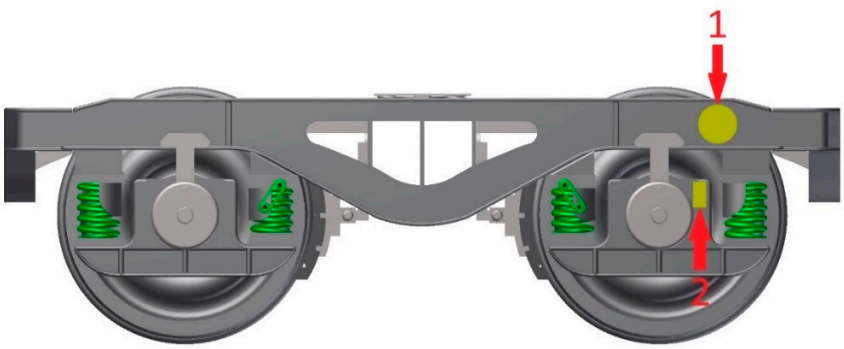

Figure 2. The place of installation of the measuring sensor and harvester on the freight wagon cart.

4.3. Modelling and Simulation Experiments

Based on the literature analysis and previous research, a pendulum-shaped harvester consisting of a moving beam with piezoelectric elements attached to it was designed (Figure 3). In order to obtain significant output power, the excitation frequency should be fixed at the resonance region of the energy harvesting system. In practice, this means adjusting the energy converting device to the frequency of the ambient vibration. Knowing the environment from which the energy will be extracted, which is the bogie of a freight car, the problem may be the absence of vibrations of resonant frequencies. Not meeting this condition does not exclude the use of a piezoelectric energy converter, but the power that can be obtained will be significantly lower.

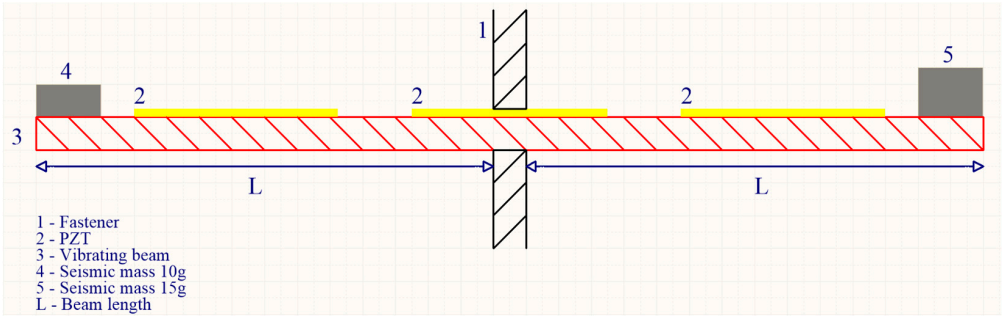

Figure 3. Scheme of the beam.

Knowing that the sesmic mass is significantly greater than the mass of the beam, the frequency formula takes the form:

$$\omega = \sqrt{\frac{k}{m}} = \sqrt{\frac{3EI}{\left(\frac{33}{140}m_1 + m_2\right)L^3}} \tag{7}$$

k—stiffness coefficient of the cantilever beam.
m—beam mass.
E—Young's modulus [Pa].
I—geometric moment of inertia of the beam [kg × m^2].
L—length of the beam [m].
m_1—mass of the beam [kg].
m_2—mass of the weight [kg].
The moment of inertia for a thin rectangular pendulum can be expressed by the formula:

$$I = \frac{Wl^3}{12} \tag{8}$$

W—width of beam [m].
l—distance of the mass from the beam attachment point.
By substituting the formula for frequency, the final formula describing the natural frequency of a beam loaded with a seismic mass is obtained [44]:

$$f = \frac{\omega}{2\pi} = \frac{1}{2\pi}\sqrt{\frac{3WEl^3}{12L^3\left(\frac{33}{140}m_1 + m_2\right)}} \tag{9}$$

Calculated according to the above formula, the natural frequency of such a pendulum is 22.9 Hz for the side loaded with 10 g mass and 15.38 Hz for the side loaded with 15 g mass. The connected three thin plates with a very small mass relative to the sum of the weights' masses of 25 g are susceptible to low-frequency vibration, which is an advantage when the converter is used in a railcar environment. In order to study the force distribution

on the surface of the piezoelectric transducer and the electrical properties of the system, a 3D model of the converter was designed and simulated in COMSOL Multiphysics. PZT-5A parameters analyzed in COMSOL Multiphysics.

Density 7750 [kg/m^3] and permittivity of free space $\varepsilon_0 = 9.191 \times 10^{-12}$ F/m.

Elasticity matrix S^E [GPa]:

$$\left[S^E\right] = \begin{bmatrix} 110.867 & 75.1791 & 75.1791 & 0 & 0 & 0 \\ 75.1791 & 120.346 & 75.0901 & 0 & 0 & 0 \\ 75.1791 & 75.0901 & 120.346 & 0 & 0 & 0 \\ 0 & 0 & 0 & 21.0526 & 0 & 0 \\ 0 & 0 & 0 & 0 & 21.0526 & 0 \\ 0 & 0 & 0 & 0 & 0 & 22.5734 \end{bmatrix} \quad (10)$$

Piezoelectric strain matrix d [10^{-12} C/N]:

$$[d] = \begin{bmatrix} 0 & 0 & -5.35116 \\ 0 & 0 & -5.35116 \\ 0 & 0 & 15.7835 \\ 0 & 0 & 0 \\ 0 & 12.2947 & 0 \\ 12.2947 & 0 & 0 \end{bmatrix} \quad (11)$$

Permittivity at constant strain matrix ε^T:

$$\left[\varepsilon^T\right] = \begin{bmatrix} 1730\varepsilon_0 & 0 & 0 \\ 0 & 1730\varepsilon_0 & 0 \\ 0 & 0 & 1700\varepsilon_0 \end{bmatrix} \quad (12)$$

The simulations carried out using COMSOL software were aimed at obtaining information on the stresses occurring on the surface of the transducers that could lead to their failure and on the voltage response of the designed model to the vibration frequency excitation from 1 Hz to 30 Hz.

The impact of vibrations with variable frequency up to 30 Hz on the piezoelectric transducer may cause local stresses at the level from 18.5 to over 220 N/m^2. This design of the vibration system allows the appearance of large amplitudes of pendulum deflections. The software generates solutions in a graphical form showing the most exposed areas, as shown in Figures 4 and 5.

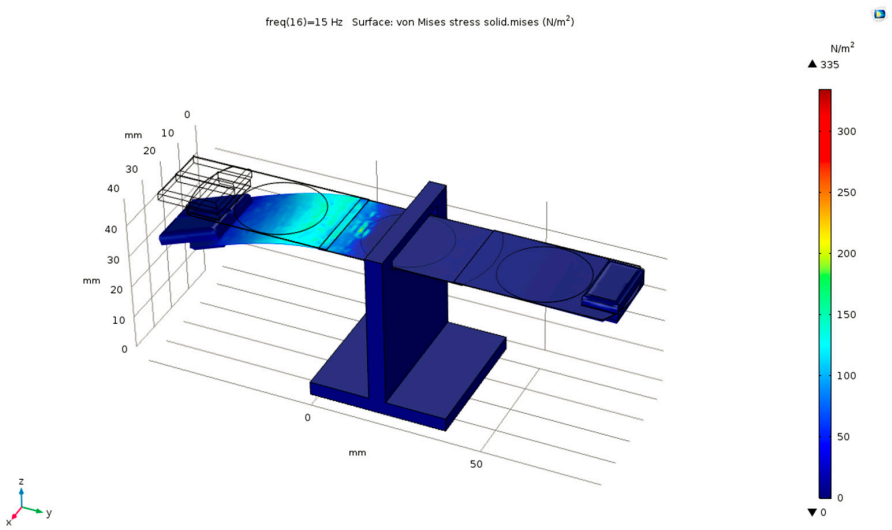

Figure 4. Stress distribution on the converter arm surface at 15 Hz vibration frequency.

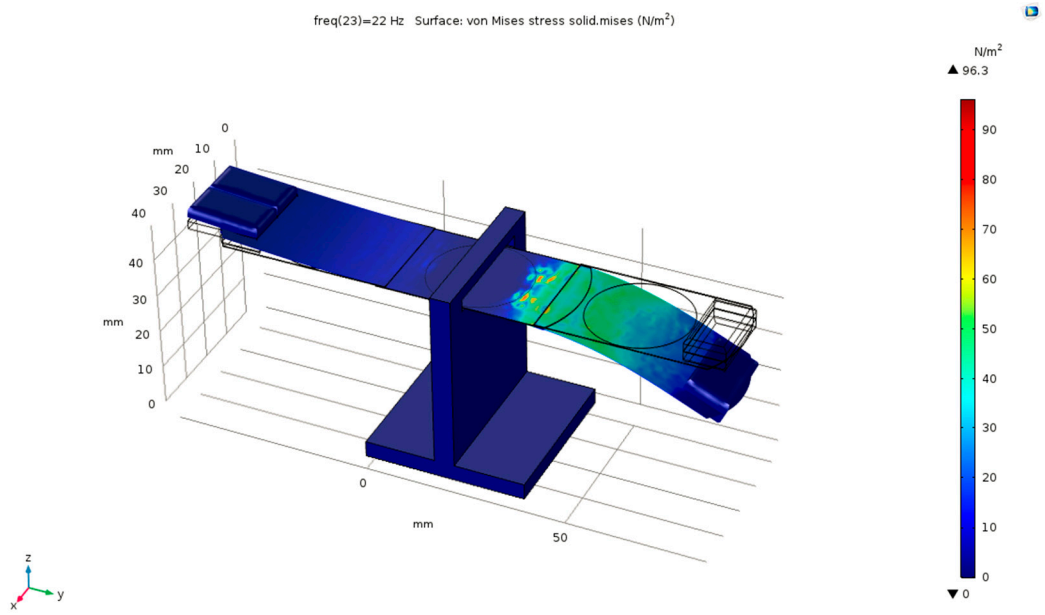

Figure 5. Stress distribution on the converter arm surface at 22 Hz vibration frequency.

The model was subjected to analysis of the response to a force forcing directed parallel to the Z axis in order to model the voltage appearing on the surface of the piezoelectric elements. For the converter simulated, the application of force at 30 Hz to the piezoelectric transducers generates a potential of 20.1 V at the terminals of the attached 25,000 Ω resistor, which is equivalent to a current flow of 804 μA, and the power dissipated at the resistor is 16.16 mW.

Figure 6 shows the distribution of forces on the harvester arms depending on the frequency of excitations. In turn, the voltage across the load is shown in Figure 7.

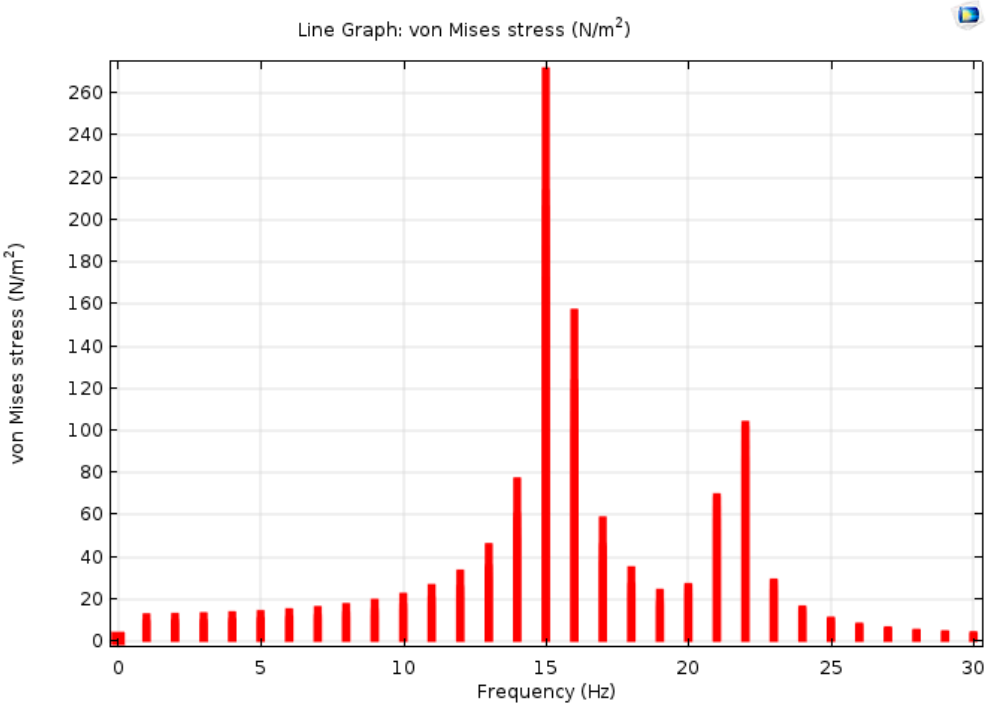

Figure 6. The value of forces acting on the harvester arms depending on the frequency of excitations.

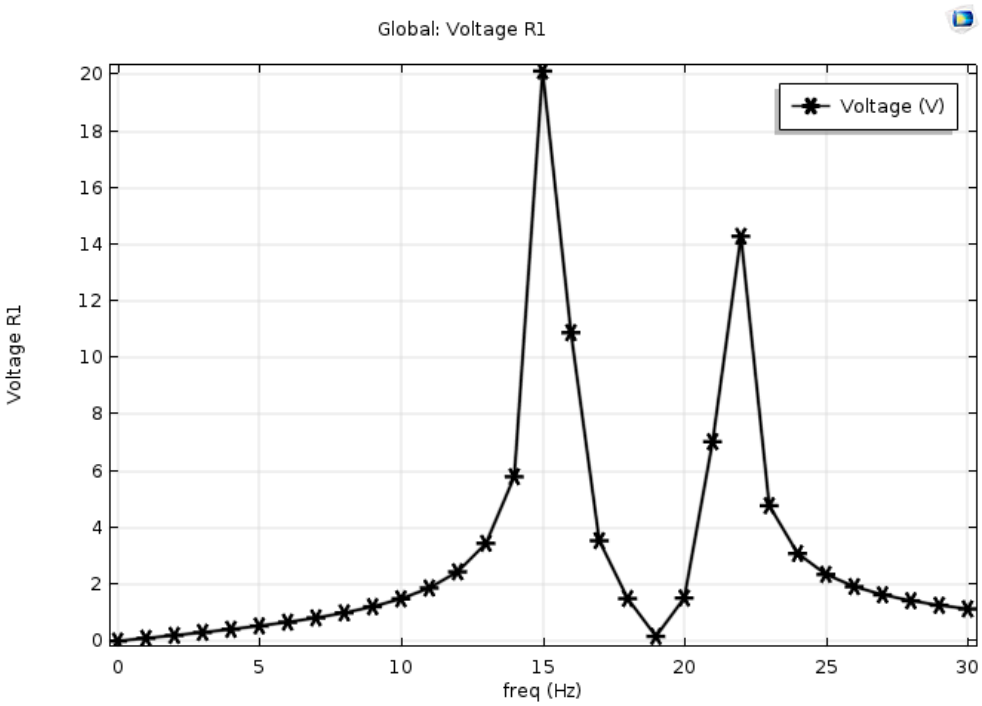

Figure 7. Voltage across the harvester load resistor.

5. Results

Simulations carried out with COMSOL software were aimed at obtaining information about the correctness of the operation of the designed piezoelectric converter. The locations of the highest stresses, indicated by the program, were supposed to help with the appropriate localization of the piezoelectric element. The maximum voltage values obtained from the simulation were recorded on the 25 kΩ resistor terminals. Next, an actual converter model was fabricated, consisting of three brass plates containing 27 mm wide piezoelectric elements connected together. This resulted in a pendulum with a total length of 116 mm. Two 5 g weights were attached to one end of the beam and three weights of 5 g each were attached to the other end. The outputs of piezoelectric elements were connected to full-wave rectifiers, to which an energy store in the form of 220 µF electrolytic capacitor and 25 kΩ resistor was connected. The electrical scheme of the tested power unit is presented in Figure 8. This converter was tested in the laboratory to determine the voltage response as a function of vibration frequency (Figure 9).

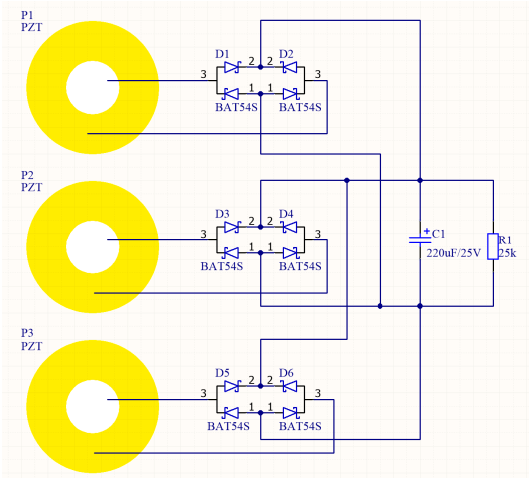

Figure 8. Electrical diagram of the system.

(**a**) (**b**)

Figure 9. Laboratory stand for power unit parameters determination. (**a**) Measurement system; (**b**) piezoelectric harvester during the tests.

The vibration generating system made the harvester oscillate with an amplitude of 1 mm and frequencies shown in Table 2. The table also shows the voltage value measured on the load after 10 s of vibration.

Table 2. Measured values of voltage and frequency.

Frequency [Hz]	Output Voltage [V]
7.02	0.45
7.95	0.56
9.30	0.66
10.30	1.07
11.20	1.98
12.20	5.22
13.2	6.19
14.2	18.41
14.65	8.9
15.00	7.42

Figure 10 shows the value of voltage to which the circuit charges the capacitor, at different vibration frequencies. When we compare the values obtained from laboratory tests and simulations (Figure 7), we see a great convergence. In both cases, the voltage rises sharply above 18 V, near the resonance frequency. For a vibration frequency of 14.2 Hz, the harvester charged a 220 uF capacitor to 18 V in only 10 s, an additional load of 25,000 Ω, this is shown in Figure 11b. The voltage value on the unloaded harvester at 14.2 Hz vibration is shown in Figure 11a.

The tests carried out in the laboratory confirmed the correct operation of the actual harvester model. The purpose of the designed converter is to obtain energy from vibrations generated by a moving freight train. The energy recovered in this way should be stored in an appropriate size energy storage, and then used by the communication and measurement module. The task of such a module would be to measure the bearing temperature of the wheelset axle and send it to the central unit by means of low-energy radio transmission.

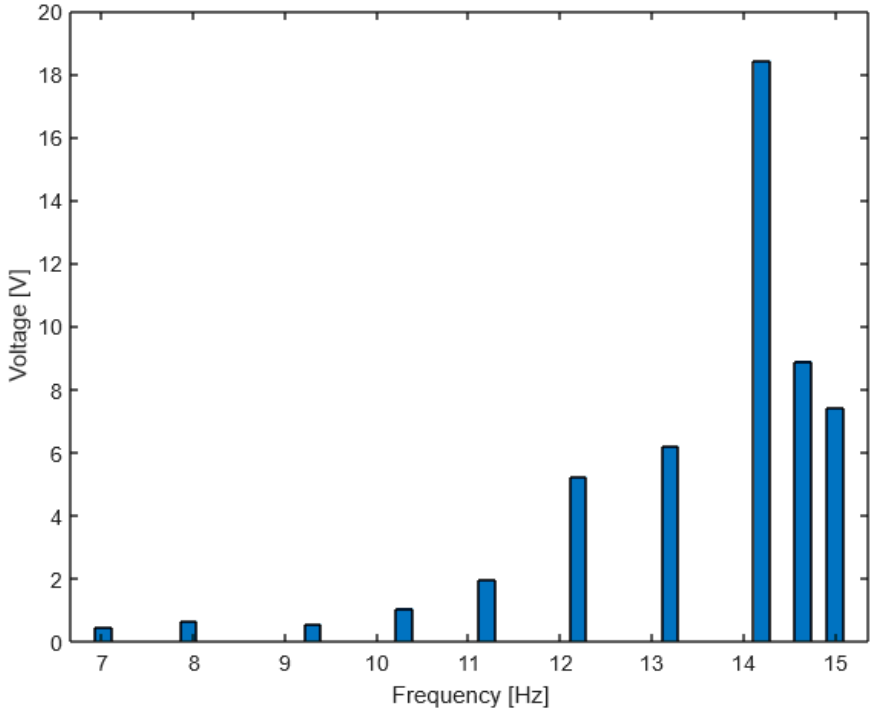

Figure 10. Voltage on the capacitor after a charging time of 10 s for different frequencies.

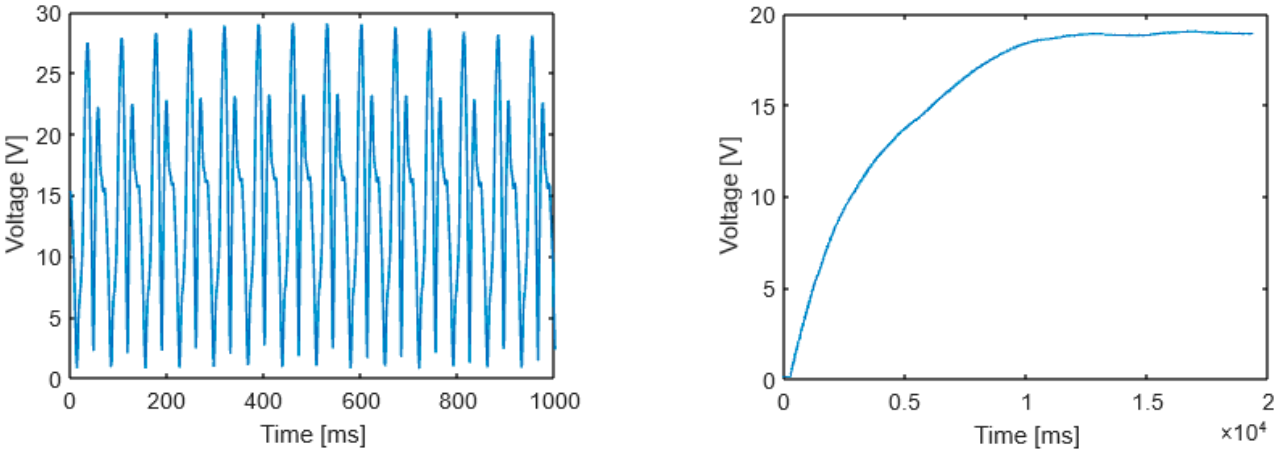

(**a**) (**b**)

Figure 11. Output voltage from harvester during 14 Hz vibration. (**a**) Voltage of an unloaded harvester; (**b**) output voltage during capacitor charging.

The converter was tested in the target environment. For this purpose, an electrical test system was made to measure the generated voltage, which was then attached to a 25TN bogie of a freight train car. Each of the piezoelectric transducers was connected to a rectifier bridge consisting of Schottke diodes. Laboratory tests showed that the harvester, set in vibration, charged the 220 µF capacitor to a sufficiently high voltage during 10 s, so the energy storage capacity was increased to 470 µF in the tested system. The electrical load for the system remained a 25,000 Ω resistor, so as to reflect the load value adopted for the simulation in COMSOL and in the laboratory. The real piezoelectric harvester is presented on Figure 12.

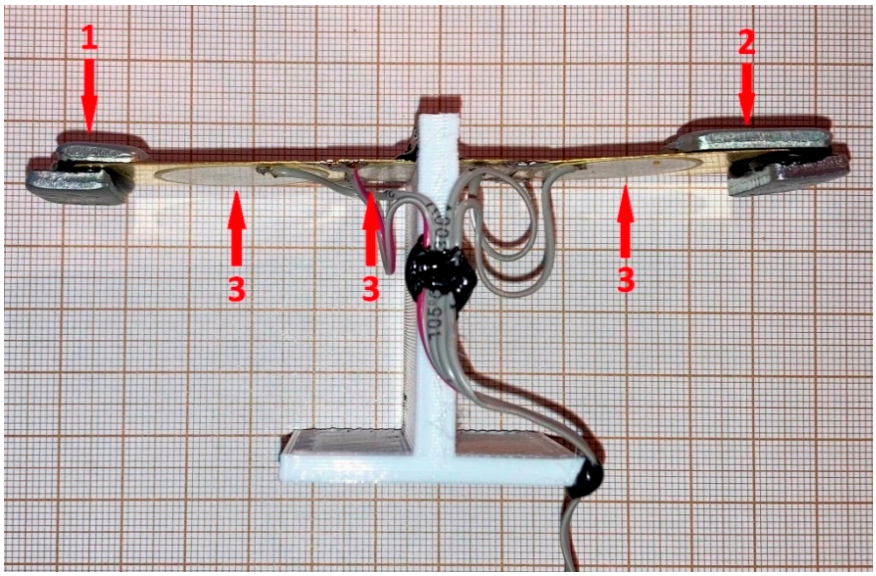

Figure 12. The real converter prepared for testing on a freight train (1—mass 10 g, 2—mass 15 g, 3—piezoelectric PZT elements).

The voltage measurement was carried out using an 8-bit ADC converter of the ESP32-SOLO module, which additionally had 4 MB of non-volatile flash memory, in which the measured values were saved. The 8bit resolution is sufficient for the measurement of direct voltage ensuring the ability to save 512 samples in the 4 MB memory. An additional 1000 mAh lithium-polymer battery LP663245 with a rated voltage of 3.7 V was used to power the measuring system. The used battery provided power to the system for 12 h of train travel. However, the ESP module memory allowed to save samples of the measured voltage for only 8 h and 30 min. The voltage measurement was performed every 60 s. The measuring system with the transducer was placed in a round, plastic housing, and then the whole was firmly attached to the frame of an intermodal freight train wagon (Figure 13). The intermodal wagon was loaded with a 20 t container. During the test, samples were recorded for 8.5 h during which the train traveled 408 km from Warsaw to Katowice. During this time, the train had two stops, from minutes 165 to 220 and from 305 to 340. The average speed of the train during the journey was 58 km per h, the maximum was 90 km/h.

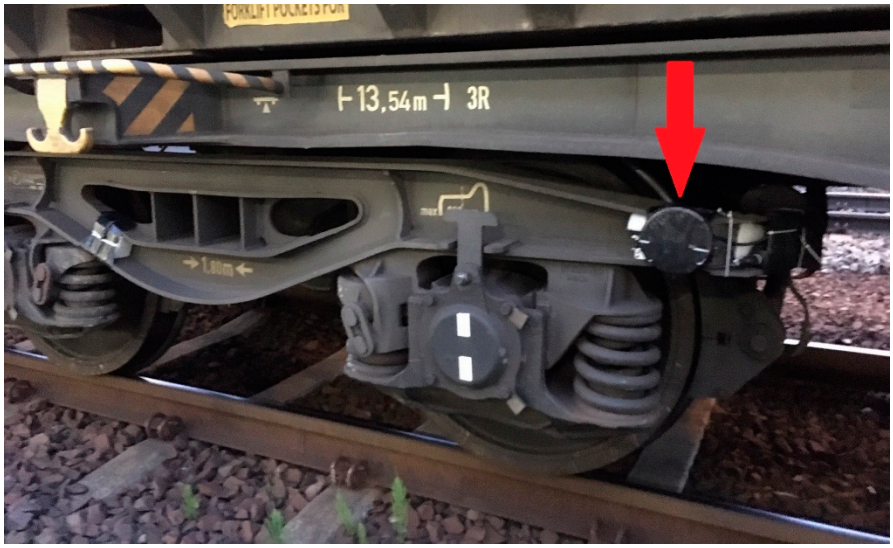

Figure 13. The converter is mounted on the 25TN bogie frame.

After removing the system from the bogie frame, the ESP module memory was read. There were 512 samples of the voltage value in the memory. From the values of the voltage samples, the intensity of the flowing current and its power was calculated, which is presented in the diagram below. The highest recorded voltage value is for sample 356 and is 2.12 V, which corresponds to the flowing current of 0.084 mA and the power of 0.179 mW generated on the resistor. The power outpu generated by the converter during the test is presented on Figure 14.

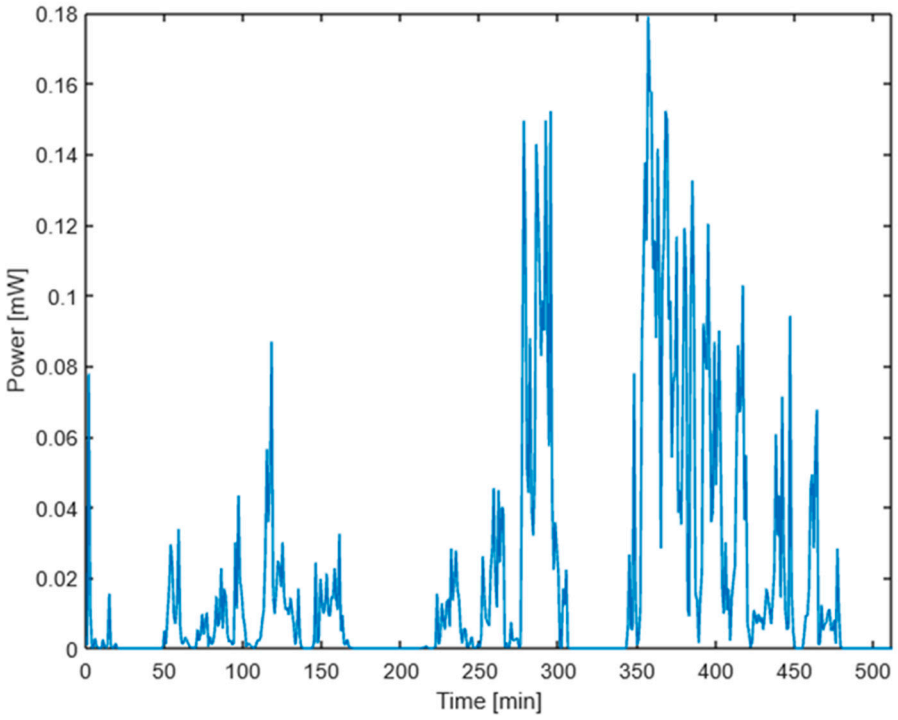

Figure 14. The value of the power generated by the energy converter for each recorded sample.

6. Discussion

The calculated vibration frequency of a freight car bogie for 50 km/h is 4.8 Hz, and for 100 km/h it is 9.6 Hz (Equations (5) and (6)). Both of these frequencies are below the resonant frequency of the harvester. As a result, the obtained values of the voltage generated by the tested converter in the real system are lower than those from the simulation and laboratory tests. The maximum value of the recorded voltage from the train vibrations is 2.12 V, which corresponds to the instantaneous power of 179 µW, on the resistor. These values correspond to the power of the harvester simulation for vibrations with a frequency ranging from 4 to 6 Hz. The single higher voltage values observed for the real system result from the momentary higher speed of the train or from the unevenness of the railway tracks, which contribute to non-periodic vibrations of the bogie. By storing energy from the environment in energy storage with a low self-discharge current, it is possible to accumulate a sufficient amount of charge to provide power when the communication system wakes up, to measure a physical quantity, e.g., temperature, and then send the measured data using a low-energy communication protocol. After the energy stored in the storage is used up, the system should go into standby mode and be powered by other sources, for example, a battery. The sleep–wake cycle of the device may depend on the rate at which the energy reservoir is charged by the piezoelectric converter, or be defined as a constant time value. The Table 3 summarizes the data of four modules enabling wireless communication using Bluetooth Low Energy (BLE). These modules can be used as a communication and measurement system, additionally powered by a piezoelectric converter.

Table 3. Data table of four modules enabling wireless communication using Bluetooth Low Energy (BLE) technology.

Communication Module	Supply Voltage [V]	Current Consumption		Type of Wireless Communication
		Sleep Mode [μA]	Broadcasting Mode [mA]	
ESP32-SOLO-1	3–3.6 V	0.05	1100	BLE, Wi-Fi
nRF52833	1.7–3.6 V	2.6	6.0	BLE
nRF52840	1.7–5.5 V	2.0	4.8	BLE
nRF5340	3–3.6 V	1.8	3.2	BLE

The energy balance calculations were made for the communication system powered from the battery, treating the piezoelectric converter as an additional system extending the working time of the sensor mounted on the railway car. The calculations do not take into account the energy taken from the environment, because its amount depends on too many factors. It should be assumed that the use of a harvester will extend the working time of the system. The analysis of the energy balance for the nRF52840 communication module is presented below. The interval of sending data every minute and the duration of transmission per second were assumed. The calculations do not take into account the power consumption for servicing other sensor peripherals, only the energy consumption for BLE transmission. The average current consumption can be determined from the following formula:

$$i_{AV} = \frac{i_T T_T + i_{SLP} T_{SLP}}{T_T + T_{SLP}} \quad (13)$$

i_T—current consumption in broadcasting mode [A].
i_{SLP}—current consumption in sleep mode [A].
T_T—time in broadcasting mode [s].
T_{SLP}—time in sleep mode [s].
i_{AV}—average current [A].

Since the system will be in sleep mode most of the time, it can be assumed that $T_{SLP} >> T_T$, so the above formula can be simplified to the following form:

$$i_{AV} = \frac{i_T T_T}{T_{SLP}} + i_{SLP} = \frac{0.0048\ \text{A} \times 1\ \text{s}}{599\ \text{s}} + 0.000002\ \text{A} = 0.00001\ \text{A} = 10\ \mu\text{A} \quad (14)$$

The working time of the module when powered by a 1000 mAh battery can be expressed as:

$$T_B = \frac{C_{BAT}}{i_{AV}} = \frac{1\ \text{Ah}}{0.00001\ \text{A}} = 100{,}000\ \text{h} = \sim 11\ \text{years} \quad (15)$$

T_B—total operating time of the battery powered system [h].
C_{BAT}—battery capacity [Ah].
i_{AV}—average current [A].

By analyzing the samples from 350 to 410 in Figure 14, corresponding to one hour of train travel, we can determine the generator's current efficiency at that time. The average value of the current flowing through the resistor is 0.0492 mA, which corresponds to the harvester's current efficiency of 0.0492 mAh and power output of 60 μW. Calculating how much time it will extend the operation of the system, energy obtained from the environment for 11 years:

$$T_H = \frac{\left(\frac{T_B}{24\ \text{h}}\right) \times C_H}{i_{AV}} = \frac{\left(\frac{100{,}000\ \text{h}}{24\ \text{h}}\right) \times 0.0000492\ \text{Ah}}{0.00001\ \text{A}} = 20{,}500\ \text{h} = \sim 2.3\ \text{years} \quad (16)$$

T_B—total operating time of battery powered system [h].
T_H—time of additional operation of the system powered by the harvester [h].

C_H—harvester current efficiency [Ah].
i_{AV}—average current consumed [A].

$$T_C = T_B + T_H = 100,000\text{ h} + 20,500\text{ h} = 120,500\text{ h} = \sim 13.3\text{ years} \quad (17)$$

TC—total system operation time [h].

Table 4 presents a comparison of performance parameters of piezoelectric harvesters. We see that the described harvester is characterized by a relatively low frequency of work vibrations only the harvester presented in 31 works at similar frequencies. It should be noted that the first resonance frequency of constructed harvester is equal to 14 Hz. The frequencies of (bogie) vibrations that may occur at standard train speeds are 4–10 Hz. However, due to higher train speeds (which is possible for passenger trains) or due to uneven track conditions the vibration frequencies may increase. It is known that the operation of the mechanical system in vibrations close to the resonant frequency causes high stress on the structure and may lead to its destruction. Therefore, our harvester operates below the resonance frequency. Thanks to this, we guarantee long-term and failure-free work in real conditions. On the other hand, thanks to the relatively low quality factor of the harvester circuit of fit it is possible to work efficiently even at frequencies lower than the resonance one. Comparing the power output of the presented harvesters, it can be seen that the presented system is characterized by a relatively high power. The solution presented in 34 has a much higher power, but this is a simulation study. Confirmed in real research, the pendulum harvester presented in 31 obtains a power density of 40 uW/cm^3, which is close to the power achieved by our power system.

Table 4. Parameter comparison of the piezoelectric harvesters.

Shape of Harvester	References	Application	Frequency Vibration [Hz]	Power Output [μW]
spring-mass oscilator	32	train	80	2
cantilever	60	universal	229	0.27
spring-mass oscilator	34	train	16	6000 simulation
pendulum	31	train	3–6	40 μW/cm^3
pendulum	presented	train	4–10	60

Knowing that the energy stored in the battery is enough for about 11 years of system operation, we can assume that if the harvester generates energy for only one hour every day, it will extend the operation time of the entire device by 20%. Obviously, this is the result in terms of ideal conditions, in which the following factors are not taken into account: the influence of temperature changes on the current consumed by the system, the slowing down of chemical processes in the battery, the leakage of current occurring in peripheral systems, and the current required for the supply of peripherals. In real conditions, the working time of the device powered by the battery will be shorter due to the use of a piezoelectric harvester, this effect can be reduced and the device's operation can be significantly extended. For this reason, systems that obtain energy from the environment that can extend the operating time of such devices are of great interest to designers of Internet of Things devices.

7. Conclusions

In our research, we presented a power supply system dedicated to WSN nodes monitoring the temperature of the axle box of a freight car. The average output power of the system is 60.5 uW. In the case of storing energy and transmitting data to the system hub once per minute, it allows to power an energy-efficient node for 13 years. When calculating the balance, we assumed only one hour of operation of the system (train travel) and the vibration frequency from 4 to 10 Hz. These are minimalistic assumptions, in real conditions the wagon is used several hours a day, and due to the unevenness of the track, the vibration

amplitudes and frequencies will be higher than assumed. In our research, we prove that by using a piezoelectric harvester it is possible to extend the life of the measuring node by 20% in comparison with power systems based only on batteries. Using an inexpensive and available piezoelectric material such as PZT, we were able to build a compact pendulum harvester that even at low vibration frequencies is able to significantly increase the operating time of the measurement node.

Author Contributions: Conceptualization, M.K. and B.D.; methodology, J.S.; software, M.K.; validation, B.D. and M.K.; formal analysis, B.D. and M.K.; investigation; writing—original draft preparation, M.K., J.S. and B.D. All authors have read and agreed to the published version of the manuscript.

Funding: This research received no external funding.

Conflicts of Interest: The authors declare no conflict of interest.

References

1. Fraga-Lamas, P.; Fernández-Caramés, T.M.; Castedo, L. Towards the Internet of Smart Trains: A Review on Industrial IoT-Connected Railways. *Sensors* **2017**, *17*, 1457. [CrossRef] [PubMed]
2. Bernal, E.; Spiryagin, M.; Cole, C. Onboard Condition Monitoring Sensors, Systems and Techniques for Freight Railway Vehicles: A Review. *IEEE Sens. J.* **2019**, *19*, 4–24. [CrossRef]
3. Zhang, J.; Huang, W.; Zhang, W.; Li, F.; Du, Y. Train-Induced Vibration Monitoring of Track Slab under Long-Term Temperature Load Using Fiber-Optic Accelerometers. *Sensors* **2021**, *21*, 787. [CrossRef] [PubMed]
4. Ye, Y.; Zhang, J.; Liang, H. An Acoustic-Based Recognition Algorithm for the Unreleased Braking of Railway Wagons in Marshalling Yards. *IEEE Access* **2020**, *8*, 120295–120308. [CrossRef]
5. Kowarik, S.; Hussels, M.-T.; Chruscicki, S.; Münzenberger, S.; Lämmerhirt, A.; Pohl, P.; Schubert, M. Fiber Optic Train Monitoring with Distributed Acoustic Sensing: Conventional and Neural Network Data Analysis. *Sensors* **2020**, *20*, 450. [CrossRef] [PubMed]
6. Hosseinkhani, A.; Younesian, D.; Eghbali, P.; Moayedizadeh, A.; Fassih, A. Sound and Vibration Energy Harvesting for Railway Applications: A Review on Linear and Nonlinear Techniques. *Energy Rep.* **2021**, *7*, 852–874. [CrossRef]
7. Gao, M.Y.; Wang, P.; Cao, Y.; Chen, R.; Liu, C. A Rail-Borne Piezoelectric Transducer for Energy Harvesting of Railway Vibration. *J. Vibroeng.* **2016**, *18*, 4647–4663. [CrossRef]
8. Tianchen, Y.; Jian, Y.; Ruigang, S.; Xiaowei, L. Vibration Energy Harvesting System for Railroad Safety Based on Running Vehicles. *Smart Mater. Struct.* **2014**, *23*, 125046. [CrossRef]
9. Wischke, M.; Masur, M.; Kröner, M.; Woias, P. Vibration Harvesting in Traffic Tunnels to Power Wireless Sensor Nodes. *Smart Mater. Struct.* **2011**, *20*, 085014. [CrossRef]
10. Nelson, C.A.; Platt, S.R.; Albrecht, D.; Kamarajugadda, V.; Fateh, M. Power Harvesting for Railroad Track Health Monitoring Using Piezoelectric and Inductive Devices. In Proceedings of the Active and Passive Smart Structures and Integrated Systems 2008, San Diego, CA, USA, 18 April 2008; SPIE: Bellingham, WA, USA, 2008; Volume 6928, pp. 198–206.
11. Li, J.; Jang, S.; Tang, J. Implementation of a Piezoelectric Energy Harvester in Railway Health Monitoring. In Proceedings of the Sensors and Smart Structures Technologies for Civil, Mechanical, and Aerospace Systems 2014, San Diego, CA, USA, 8 March 2014; SPIE: Bellingham, WA, USA, 2014; Volume 9061, pp. 711–718.
12. Wang, J.; Shi, Z.; Xiang, H.; Song, G. Modeling on Energy Harvesting from a Railway System Using Piezoelectric Transducers. *Smart Mater. Struct.* **2015**, *24*, 105017. [CrossRef]
13. Jung, I.; Shin, Y.-H.; Kim, S.; Choi, J.; Kang, C.-Y. Flexible Piezoelectric Polymer-Based Energy Harvesting System for Roadway Applications. *Appl. Energy* **2017**, *197*, 222–229. [CrossRef]
14. European Union. Directive (EU) 2016/798 of the European Parliament and of the Council of 11 May 2016 on Railway Safety (Text with EEA Relevance). *Off. J. Eur. Union* **2016**, *OJ L 138*, 102–144.
15. Lazarescu, M.T.; Poolad, P. Asynchronous Resilient Wireless Sensor Network for Train Integrity Monitoring. *IEEE Internet Things J.* **2021**, *8*, 3939–3954. [CrossRef]
16. Xu, H.; Jin, X.; Kong, F.; Deng, Q. Maximizing the Lifetime of Wireless Sensor Networks in Trains for Monitoring Long-Distance Goods Transportation. *Int. J. Distrib. Sens. Netw.* **2017**, *13*, 1550147717707895. [CrossRef]
17. Philipose, A.; Rajesh, A. Investigation on Energy Efficient Sensor Node Placement in Railway Systems. *Eng. Sci. Technol. Int. J.* **2016**, *19*, 754–768. [CrossRef]
18. Brezulianu, A.; Aghion, C.; Hagan, M.; Geman, O.; Chiuchisan, I.; Balan, A.-L.; Balan, D.-G.; Balas, V.E. Active Control Parameters Monitoring for Freight Trains, Using Wireless Sensor Network Platform and Internet of Things. *Processes* **2020**, *8*, 639. [CrossRef]
19. He, W.; Shi, W.; Le, J.; Li, H.; Ma, R. Geophone-Based Energy Harvesting Approach for Railway Wagon Monitoring Sensor With High Reliability and Simple Structure. *IEEE Access* **2020**, *8*, 35882–35891. [CrossRef]
20. Zuo, J.; Dong, L.; Ding, J.; Wang, X.; Diao, P.; Yu, J. Design and Validation of a Self-Powered Device for Wireless Electronically Controlled Pneumatic Brake and Onboard Monitoring in Freight Wagons. *Energy Convers. Manag.* **2021**, *239*, 114229. [CrossRef]

21. Pan, Y.; Liu, F.; Jiang, R.; Tu, Z.; Zuo, L. Modeling and Onboard Test of an Electromagnetic Energy Harvester for Railway Cars. *Appl. Energy* **2019**, *250*, 568–581. [CrossRef]
22. De Pasquale, G.; Somà, A.; Zampieri, N. Design, Simulation, and Testing of Energy Harvesters With Magnetic Suspensions for the Generation of Electricity From Freight Train Vibrations. *J. Comput. Nonlinear Dyn.* **2012**, *7*, 041011. [CrossRef]
23. Gao, M.; Cong, J.; Xiao, J.; He, Q.; Li, S.; Wang, Y.; Yao, Y.; Chen, R.; Wang, P. Dynamic Modeling and Experimental Investigation of Self-Powered Sensor Nodes for Freight Rail Transport. *Appl. Energy* **2020**, *257*, 113969. [CrossRef]
24. Cho, J.Y.; Jeong, S.; Jabbar, H.; Song, Y.; Ahn, J.H.; Kim, J.H.; Jung, H.J.; Yoo, H.H.; Sung, T.H. Piezoelectric Energy Harvesting System with Magnetic Pendulum Movement for Self-Powered Safety Sensor of Trains. *Sens. Actuators A Phys.* **2016**, *250*, 210–218. [CrossRef]
25. Beagles, A. *SUSTRAIL Concluding Technical Report*; Int. Union Railways: Paris, France, 2015; Volume 1. Available online: http://www.sustrail.eu (accessed on 7 January 2022).
26. Lopes, M.V.; Eckert, J.J.; Martins, T.S.; Santos, A.A. Optimization of EH Multi-Beam Structures for Freight Car Vibration. *IFAC-PapersOnLine* **2018**, *51*, 849–854. [CrossRef]
27. Lopes, M.V.; Eckert, J.J.; Martins, T.S.; Santos, A.A. Optimizing Strain Energy Extraction from Multi-Beam Piezoelectric Devices for Heavy Haul Freight Cars. *J. Braz. Soc. Mech. Sci. Eng.* **2019**, *42*, 59. [CrossRef]
28. Covaci, C.; Gontean, A. Piezoelectric Energy Harvesting Solutions: A Review. *Sensors* **2020**, *20*, 3512. [CrossRef]
29. Elahi, H.; Eugeni, M.; Fune, F.; Lampani, L.; Mastroddi, F.; Paolo Romano, G.; Gaudenzi, P. Performance Evaluation of a Piezoelectric Energy Harvester Based on Flag-Flutter. *Micromachines* **2020**, *11*, 933. [CrossRef]
30. Directive 2011/65/EU of the European Parliament and of the Council on the Restriction of the Use of Certain Hazardous Substances in Electrical and Electronic Equipment. *Off. J. Eur. Union* **2011**, *OJ*, L174.
31. Rezaeisaray, M.; Gowini, M.E.; Sameoto, D.; Raboud, D.; Moussa, W. Wide-Bandwidth Piezoelectric Energy Harvester with Polymeric Structure. *J. Micromech. Microeng.* **2014**, *25*, 015018. [CrossRef]
32. Leppe-Nerey, J.R.; Nicho, M.E.; Sierra-Espinosa, F.Z.; Hernández-Guzmán, F.; Fuentes-Pérez, M. Experimental Study of Piezoelectric Polymeric Film as Energy Harvester. *Mater. Sci. Eng. B* **2021**, *272*, 115366. [CrossRef]
33. Kim, M.; Yun, K.-S. Helical Piezoelectric Energy Harvester and Its Application to Energy Harvesting Garments. *Micromachines* **2017**, *8*, 115. [CrossRef]
34. Baek, C.; Yun, J.H.; Wang, J.E.; Jeong, C.K.; Lee, K.J.; Park, K.-I.; Kim, D.K. A Flexible Energy Harvester Based on a Lead-Free and Piezoelectric BCTZ Nanoparticle–Polymer Composite. *Nanoscale* **2016**, *8*, 17632–17638. [CrossRef]
35. Mokhtari, F.; Shamshirsaz, M.; Latifi, M.; Foroughi, J. Nanofibers-Based Piezoelectric Energy Harvester for Self-Powered Wearable Technologies. *Polymers* **2020**, *12*, 2697. [CrossRef]
36. Lee, H.J.; Zhang, S.; Bar-Cohen, Y.; Sherrit, S. High Temperature, High Power Piezoelectric Composite Transducers. *Sensors* **2014**, *14*, 14526–14552. [CrossRef]
37. Khazaee, M.; Rezaniakolaie, A.; Rosendahl, L. A Broadband Macro-Fiber-Composite Piezoelectric Energy Harvester for Higher Energy Conversion from Practical Wideband Vibrations. *Nano Energy* **2020**, *76*, 104978. [CrossRef]
38. Peddigari, M.; Kim, G.-Y.; Park, C.H.; Min, Y.; Kim, J.-W.; Ahn, C.-W.; Choi, J.-J.; Hahn, B.-D.; Choi, J.-H.; Park, D.-S.; et al. A Comparison Study of Fatigue Behavior of Hard and Soft Piezoelectric Single Crystal Macro-Fiber Composites for Vibration Energy Harvesting. *Sensors* **2019**, *19*, 2196. [CrossRef]
39. Wilson, S.A.; Rayner, P.J.; Gore, J.; Bowles, A.R.; McBride, R.C. A Comparative Study of Ultrasonic Micro-Motors Based on Single Crystal PMN-PT and Polycrystalline PZT Ceramics. In Proceedings of the Industrial and Commercial Applications of Smart Structures Technologies 2008, San Diego, CA, USA, 19 March 2008; Volume 6930, p. 693013.
40. Dziadak, B.; Makowski, Ł.; Michalski, A. Survey of Energy Harvesting Systems for Wireless Sensor Networks in Environmental Monitoring. *Metrol. Meas. Syst.* **2016**, *23*, 495–512. [CrossRef]
41. Khan, M.B.; Kim, D.H.; Han, J.H.; Saif, H.; Lee, H.; Lee, Y.; Kim, M.; Jang, E.; Hong, S.K.; Joe, D.J.; et al. Performance Improvement of Flexible Piezoelectric Energy Harvester for Irregular Human Motion with Energy Extraction Enhancement Circuit. *Nano Energy* **2019**, *58*, 211–219. [CrossRef]
42. Tian, Y.; Li, G.; Yi, Z.; Liu, J.; Yang, B. A Low-Frequency MEMS Piezoelectric Energy Harvester with a Rectangular Hole Based on Bulk PZT Film. *J. Phys. Chem. Solids* **2018**, *117*, 21–27. [CrossRef]
43. Romaniszyn, Z. *Trolley Chassis of Railway Vehicles*; Publishing House of the Institute of Railway Vehicles: Cracow, Poland, 2005.
44. Yu, H.; Zhou, J.; Deng, L.; Wen, Z. A Vibration-Based MEMS Piezoelectric Energy Harvester and Power Conditioning Circuit. *Sensors* **2014**, *14*, 3323–3341. [CrossRef]